EMILIN1 represents a major stromal element determining human trophoblast invasion of the uterine wall

Paola Spessotto[1,*], Roberta Bulla[2,*], Carla Danussi[1], Oriano Radillo[3], Marta Cervi[1], Giada Monami[1,‡], Fleur Bossi[2], Francesco Tedesco[3], Roberto Doliana[1] and Alfonso Colombatti[1,4,5,§]

[1]Divisione di Oncologia Sperimentale 2, CRO-IRCCS, 33081 Aviano, Italy
[2]Dipartimento di Fisiologia e Patologia, University of Trieste, Trieste, Italy
[3]Laboratorio di Analisi, IRCCS Burlo Garofalo, University of Trieste, Trieste, Italy
[4]Dipartimento di Scienze e Tecnologie Biomediche, University of Udine, Udine, Italy
[5]MATI Center of Excellence, University of Udine, 35100 Udine, Italy

*These authors have contributed equally to this work
‡Present address: Department of Urology, Kimmel Cancer Center, Thomas Jefferson University, Philadelphia, PA, USA
§Author for correspondence (e-mail: acolombatti@cro.it)

Accepted 29 August 2006
Journal of Cell Science 119, 4574-4584 Published by The Company of Biologists 2006
doi:10.1242/jcs.03232

Summary

The detection of EMILIN1, a connective tissue glycoprotein associated with elastic fibers, at the level of the ectoplacental cone and trophoblast giant cells of developing mouse embryos (Braghetta et al., 2002) favored the idea of a structural as well as a functional role for this protein in the process of placentation. During the establishment of human placenta, a highly migratory subpopulation of extravillous trophoblasts (EVT), originating from anchoring chorionic villi, penetrate and invade the uterine wall. In this study we show that EMILIN1, produced by decidual stromal and smooth muscle uterine cells, is expressed in the stroma and in some instances as a gradient of increasing concentration in the perivascular region of modified vessels. This distribution pattern is consistent with the haptotactic directional migration observed in in vitro functional studies of freshly isolated EVT and of the immortalized HTR-8/SVneo cell line of trophoblasts. Function-blocking monoclonal antibodies against α4-integrin chain and against EMILIN1 as well as the use of EMILIN1-specific short interfering RNA confirmed that trophoblasts interact with EMILIN1 and/or its functional gC1q1 domain via α4β1 integrin. Finally, membrane type I-matrix metalloproteinase (MT1-MMP) and MMP-2 were upregulated in co-cultures of trophoblast cells and stromal cells, suggesting a contributing role in the haptotactic process towards EMILIN1.

Supplementary material available online at
http://jcs.biologists.org/cgi/content/full/119/21/4574/DC1

Key words: EMILIN1, α4 integrin, Trophoblast, Migration, MMP

Introduction

Placenta is a newly formed tissue organized at the feto-maternal interface during pregnancy with the contribution of both the fetus and the mother. The fetal counterpart is represented by trophoblasts that cover the chorionic villi and which comprise two layers of cells. The inner layer is formed by cytotrophoblasts (CTBs) that adhere to the basal membrane of the villi. These cells mature into multinucleated syncytiotrophoblasts localized in the outer surface of the villi in direct contact with the maternal blood circulating in the intervillous space. The villous trophoblasts constitute a continuous physical barrier that allows a selective passage of nutrients and protective factors from the mother to the fetus.

Anchoring villi insert into the maternal decidua, which contributes to establish a physical interaction between the fetus and the mother. From the tip of the anchoring villi, cytotrophoblasts migrate as extravillous trophoblasts (EVTs) into the decidua. Endovascular trophoblasts represent a special subpopulation of EVTs that colonize the spiral arteries moving against the blood flow and partially replacing the endothelial cells. Zhou et al. (Zhou et al., 1997) and Bulla et al. (Bulla et al., 2005) have shown that endovascular trophoblasts replace the endothelium via a non-destructive process leading the trophoblasts to adhere to the extravascular side of endothelial cells and to migrate through the endothelium using vascular endothelial (VE)-cadherin for cell-cell interaction. Other EVTs invade the interstitium of the decidua, reaching the inner-third of the myometrium. These cells tend to accumulate around the spiral arteries and contribute to the vascular remodeling characterized by progressive loss of smooth muscle cells and deposition of fibrinoid material on the arterial wall. This process leads to an increased diameter and decreased resistance of the spiral arteries and provides a means of steady perfusion of the placental sinusoids with maternal blood (Graham and Lala, 1992; Kaufmann and Castellucci, 1997; Aplin et al., 2000).

Studies directed at elucidating mechanisms that regulate EVT cell proliferation, migration and invasion have indicated that regulation is provided by a variety of factors present in the EVT cell microenvironment, including growth factors, growth

factor-binding proteins, metalloproteinases (MMPs) and extracellular matrix (ECM) components (reviewed by Norwitz et al., 2001; Hamilton et al., 1998; Campbell et al., 2003). During the differentiation of CTBs into the EVT cell lineage and invasion of the uterine wall, these cells modulate the expression of a wide range of adhesive molecules (Hamilton et al., 1998; Aplin, 1993; Damsky et al., 1992; Korhonen et al., 1991; Irving and Lala, 1995). They replace the epithelial-like receptors, e.g. E-cadherin and α6β4 integrin, with adhesion molecules typical of endothelial cells, e.g. VE-cadherin, vascular cell adhesion molecule-1 (VCAM-1), platelet-endothelial cell adhesion molecule-1 (PECAM-1), and αvβ3 and α1β1 integrins (Ilic et al., 2001). In addition, EVTs further resemble vascular cells by expressing urokinase plasminogen activator (Queenan et al., 1987) and the thrombin receptor (Even-Ram et al., 1998).

During invasion and migration of tissues and vessels, EVTs encounter obstacles similar to those that tumor cells must overcome to invade surrounding and distant tissues during the metastatic process. EVT invasiveness, while remaining largely confined to the endometrium-myometrium junction, depends on mechanisms similar to those of invasive tumor cells. Invasion in situ is regulated by locally derived factors as well as by interactions of EVT with certain ECM components through cell surface integrins (Irving and Lala, 1995). For instance, fibronectin (FN) is abundant at sites of anchoring villus formation in vivo and both maternal and trophoblast-derived FNs are present in the ECM encountered by EVT in their pathway within the decidual tissue. Thus, it was suggested that FN acts as a bridging ligand mediating anchorage and/or migratory activity following the interaction with the cognate α5β1 integrin receptor of EVTs (Ilic et al., 2001).

The aim of the present investigation was to define the role of EMILIN1, a connective tissue glycoprotein associated with elastic fibers (Doliana et al., 1999), in the process of interstitial (stromal) migration and/or invasion of EVTs. The study was prompted by a previous finding that abundant EMILIN1 mRNA is present at the level of the ectoplacental cone and trophoblast giant cells of developing mouse embryos (Braghetta et al., 2002). EMILIN1 belongs to a new family of proteins of the ECM characterized by a unique arrangement of structural domains, including a unique cysteine-rich sequence of approximately 80 amino acids at the amino-terminus, the EMI domain, an α-helical domain with high probability for coiled-coil structure formation in the central part, and a region homologous to the globular domain of C1q (gC1q domain) at the carboxyl-terminal end (Doliana et al., 1999; Colombatti et al., 2000). EMILIN1 is often observed in vivo closely adjacent to the surface of cells; it is recognized at its gC1q1 domain by the α4β1 integrin and it is able to promote tumor cell migration (Spessotto et al., 2003a).

In the present study, by using ex vivo cells and an in vitro cellular model system of trophoblast, we have identified EMILIN1 as a candidate molecule exerting a crucial role in promoting EVT migration and/or invasion from the anchoring columns into the decidualized and perivascular stroma.

Results

Immunolocalization of EMILIN1 in human placenta

The presence of EMILIN1 was documented both at the level of the chorionic villi and in decidua (Fig. 1A). No staining was

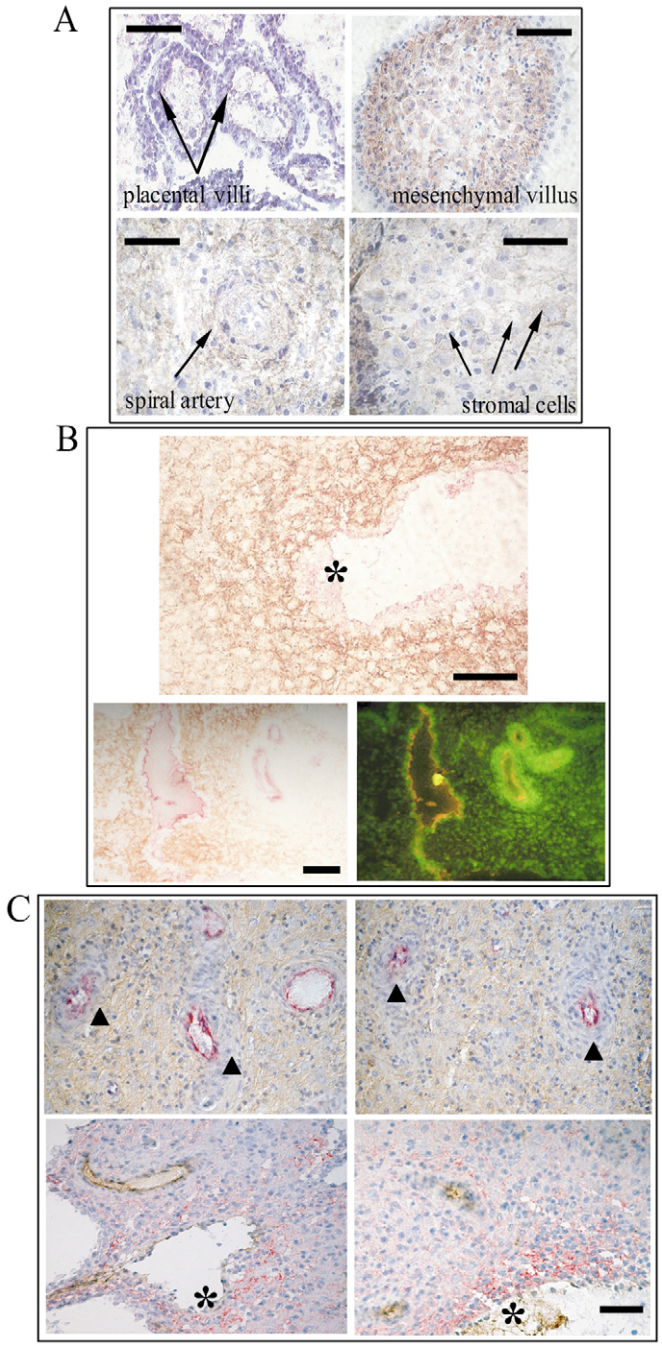

Fig. 1. Localization of EMILIN1 in first-trimester human placenta. (A) Cryostat sections of first-trimester placenta were stained with antibodies specific for EMILIN1 followed by secondary HRP-labeled antibodies and developed with DAB. The sections were counterstained with hemallum. (B) This section was immunostained for EMILIN1 (in brown) and for the presence of vWF, visualized with an alkaline-phosphatase-labeled secondary antibody, and it was not counterstained. Asterisk indicates a modified vessel; lower panel: triple staining for EMILIN1 (in brown), and cytokeratin (in green fluorescence) and vWF (in red) to visualize EVT and endothelial cells, respectively. (C) Cryostat sections of first-trimester placenta were immunostained for EMILIN1 and for the presence of vWF. Upper panel: EMILIN1 (in brown) and vWF (in pink); lower panel: EMILIN1 (in pink) and vWF (in brown). Arrowheads indicate spiral arteries and asterisks large modified vessels where the gradient distribution of EMILIN1 seems more evident. Bars, 50 μm.

seen in the sincytiotrophoblast layer and in the underlying cytotrophoblast stem cells (Fig. 1A, upper panel). The analysis of a section of an immature mesenchymal villous revealed an intensive staining in large polygonal stromal cells with vescicular nuclei and abundant cytoplasm (Fig. 1A, upper panel). In decidua EMILIN1 was expressed at low levels in proximity to apparently unmodified spiral arteries (Fig. 1A, lower panel; Fig. 1C, upper panel; supplementary material Fig. S1). Interestingly, the staining of EMILIN1 in certain areas of the decidual stroma displayed a gradient of increasing intensity towards 'modified' vessels (Fig. 1B; Fig. 1C, lower panel). This pattern was more evident in modified vessels of larger size. The EMILIN1 gradient stopped abruptly at the level of perivascular EVTs (Fig. 1B). The use of double and/or triple immunostaining better illustrated the relationship among blood vessels, EVT, stromal cells and EMILIN1 (Fig. 1B; supplementary material Fig. S1).

At the level of unmodified vessels (supplementary material Fig. S1A) EMILIN1 is distributed more evenly in the stroma as well as in the vessel media, as shown by serial z-sections (supplementary material Fig. S1B).

Cell adhesion of trophoblast cells to ECM components

The villous ECM sustains the overlaying trophoblast and supports major placental morphogenetic processes, such as remodeling and vascular development. Several ECM components are expressed in placental stroma and few were suggested to play major functional roles (Ilic et al., 2001; Damsky et al., 1992; Korhonen et al., 1991; Irving and Lala, 1995; Kilburn et al., 2000). To evaluate the pro-adhesive properties of ECM components, we used an extensive panel of purified ECM molecules and observed that HTR-8/SVneo cells bound weakly (i.e. from 15% to 25% of cell adhesion) to collagen (Col) III, Col V, fibrinogen, matrigel, tenascin, moderately well (i.e. from 26% to 49% of cell adhesion) to laminin-1 (LN-1), perlecan, Col IV, Col VI, and strongly attached (i.e. above 50% cell adhesion) to Col I, FN, vitronectin (VN), hyaluronan (HA), EMILIN1 (Fig. 2A). Several molecules that showed a weak ability to support HTR-8/SVneo adhesion were not altered or devoid of adhesive function since they actively sustained attachment of other cell types (data not shown). To investigate whether the expression of EMILIN1 in placenta could exert a specific and functional role, we examined the ability of fresh EVT cells derived from first-trimester human placentas to interact with this ECM molecule. Although with some variability, fresh EVT cells displayed a strong reactivity for EMILIN1 and FN comparable to HTR-8/SVneo cells (Fig. 2B).

gC1q1, the functional C-terminal domain of EMILIN1 (Spessotto et al., 2003a), was required and sufficient to promote cell adhesion (Fig. 2C). The specificity of the interaction was supported by the finding that a complete inhibition of HTR-8/SVneo cell attachment was obtained in the presence of the P1H4 function-blocking anti-α4-integrin antibody (Fig. 2C). The adhesion was also blocked using the monoclonal antibody (mAb) 1H2G8 mapping to the gClq1 domain, indicating that trophoblast α4β1 integrin interacts with EMILIN1 through the gC1q1 domain of the protein. FACS analyses confirmed the presence of the α4β1 integrin receptor on freshly isolated and Ck7-positive EVT cells and provided for HTR-8/SVneo cells an integrin profile corresponding to their adhesive pattern (data not shown).

In agreement with the α4β1 usage in cell adhesion to EMILIN1, there was a pronounced qualitative difference in the

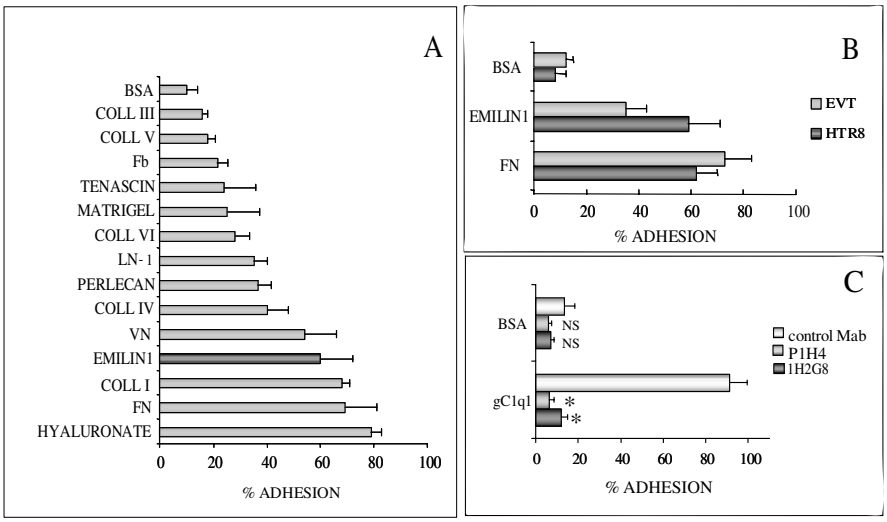

Fig. 2. Cell adhesion to ECM substrates. (A) Levels of HTR-8/SVneo cell adhesion to a selected panel of purified ECM proteins. Substrate proteins were coated at 10 μg/ml and cell adhesion was performed in the presence of 1.0 mM Mg^{2+} and 1.0 mM Ca^{2+}. Statistical tests were not performed for this descriptive adhesive analysis. (B) Adhesion of HTR-8/SVneo and freshly isolated EVT cells to EMILIN1 and FN. Four experiments were performed and mean ± s.d. reported. No significative difference was seen between EVT and HTR-8/SVneo adhesion capability on EMILIN1 and FN substrates. (C) Perturbation of HTR-8/SVneo cell attachment to gC1q1. Wells were coated with gC1q1 (10 μg/ml). The anti-EMILIN1 mAb 1H2G8 was added to the coated wells just before addition of the cells. In other instances the cells were preincubated with the anti-α4 integrin subunit mAb P1H4 for 15 minutes at 37°C and were then allowed to adhere at 37°C for 20 minutes. Data are expressed as mean ± s.d. Post-hoc comparison of control mAb versus test samples after significant ANOVA for repeated-measures main effect, Dunnet's test (n=3). *P<0.01.

morphology of cells attached to EMILIN1 compared with cells plated on FN or VN. Cells attached to FN and VN appeared well spread out on the substrate, whereas cells attached to EMILIN1 appeared much smaller, displaying wide ruffles, extending in multiple directions (supplementary material Fig. S2A). Phalloidin staining of cells spread on FN and VN revealed a high number of actin-containing stress fibers. In addition, paxillin localized to large focal contacts at the tips of stress fibers (supplementary material Fig. S2A, upper panel). Accordingly, focal adhesion kinase (FAK) also localized to focal contacts (supplementary material Fig. S2A, lower panel). By contrast, phalloidin staining of cells attached to EMILIN1 indicated that actin was mainly present along the cell periphery at the level of extended cell protrusions, reflecting a different organization status of the actin cytoskeleton compared with the cells on FN or VN; both paxillin and FAK were evenly distributed in the cell cytoplasm without any apparent focal contact formation (supplementary material Fig. S2). Focal contacts were not visible even after 3 hours of adhesion on EMILIN1 (supplementary material Fig. S2), suggesting that the different morphology initially detected at 30 minutes of adhesion was not dependent upon an incomplete occupancy of the integrin.

Trophoblast cell movement towards EMILIN1

These findings prompted us to ask whether EMILIN1 promoted efficient migration of trophoblast cells. Accordingly, as a first approach, we compared migration towards EMILIN1 versus a selected series of ECM molecules and used HTR-8/SVneo cells to determine quantitatively the substrate preference. HTR-8/SVneo cells did not migrate above background levels towards Col IV and moved poorly towards LN-1 and Col I (Fig. 3A). Instead, a significant number of cells migrated effectively as early as 5 hours towards FN-, VN- and EMILIN1-coated filters (Fig. 3A).

To obtain further insight into the motility of HTR-8/SVneo, cells were allowed to migrate under two different experimental conditions. Chamber filters were either coated with ECM molecules on their lower side to enable cells to engage in haptotactic directional migration towards the substratum-bound density gradient of adsorbed protein (McCarthy and Furcht, 1984), or coated on the upper side to evaluate the intrinsic motility of the cells in the absence of an 'ECM gradient' (a cell movement defined as 'migration'). HTR-8/SVneo cells displayed polarized migration to a similar extent (approximately 20% of migrated cells) irrespective of which side of the filter was coated with FN (Fig. 3B). In sharp contrast, EMILIN1 was able to significantly enhance directional motility when filters were coated on the lower surface (35% migration) compared with coating on the upper side (18% migration), suggesting that this protein promotes haptotaxis more efficiently than FN. The observed migratory preference displayed by HTR-8/SVneo cells was also reproduced with EVT cells that moved towards EMILIN1 with a significantly higher efficiency than towards FN (Fig. 3C). Thus, this similarity suggests the potential biological

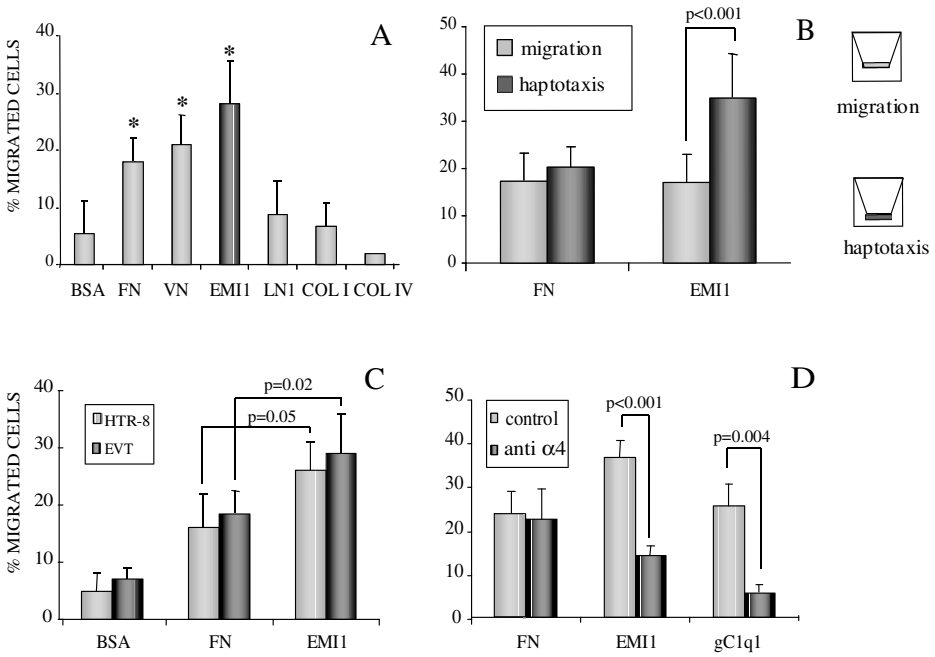

Fig. 3. Cell migration towards ECM substrates. (A) Haptotactic migration of HTR-8/SVneo towards various purified ECM substrates. The filters were coated on the lower surface with 20 μg/ml of the substrates. Data are expressed as mean ± s.d. under baseline conditions (BSA). Post-hoc comparison of BSA versus test substrates after significant ANOVA for repeated-measures main effect, Dunnet's test (n=4). *P<0.05. (B) Migration versus haptotaxis of HTR-8/SVneo cells. Filters were coated with purified FN or EMILIN-1 on their upper (migration) or lower (haptotaxis) surfaces and the cells were allowed to migrate for 5 hours. The values shown represent the mean ± s.d. of five experiments. P was calculated for values obtained in haptotactic versus migration conditions. (C) Haptotactic migration of HTR-8/SVneo and fresh EVT cells in response to FN or EMILIN1 was determined by FATIMA assay at one time point (5 hours). The mean ± s.d. of three experiments is reported. (D) The effect of the α4 function-blocking mAb P1H4 is shown. For EMILIN1 and gC1q1 P values are reported. The values shown represent the mean ± s.d. of three experiments.

significance of EMILIN1 in placentation and allowed us to consider HTR-8/SVneo similar to primary cells. The haptotactic motility towards EMILIN1 or gC1q1 was to a large extent inhibited by the addition of function-blocking α4-integrin subunit mAbs (Fig. 3D), indicating that this cellular receptor plays a crucial role.

In vitro production of EMILIN1

Based on the finding that EMILIN1 appeared to be a preferential substrate for trophoblast directional migration, we searched for the cellular source of EMILIN1. Decidual stromal cells (DSC), human umbilical vein endothelial cells (HUVEC), uterine smooth muscle cells (UtSMC) and HTR-8/SVneo cells were stained with anti-FN and anti-EMILIN1 antibodies. All cell types stained for FN, with DSC and UtSMC showing stronger positivity (Fig. 4A). By contrast, EMILIN1 was detected only in DSC and UtSMC cultures. Immunoblot analysis with specific antibodies confirmed the pattern of ECM expression (supplementary material Fig. S3A). In accordance with the results in situ on cell layers, FN was detected in several cell extracts and was absent in HTR-8/SVneo cells. EMILIN1 was only detected in cell extracts of DSC and UtSMC. Immunofluorescence staining on decidua specimens supported these data: EMILIN1 was clearly present very close and associated with vimentin-positive cells (stromal cells), indicating that these cells probably represent the principal source of EMILIN1 in vivo (Fig. 4B, supplementary material Fig. S3B). The increasing gradient of expression of EMILIN1 towards CD31-positive cells of a large vessel was also evident (supplementary material Fig. S3B). At higher magnification it was clear that staining for EMILIN1 was not detectable in the trophoblast layer and around clumps of trophoblast cells within the stroma (Fig. 4B). Taken together, these results suggest that the strong expression of EMILIN1 in areas surrounding blood vessels in vivo might be because of a prevalent secretion and deposition by DSC and in part by muscular cells when still present in the vessel walls.

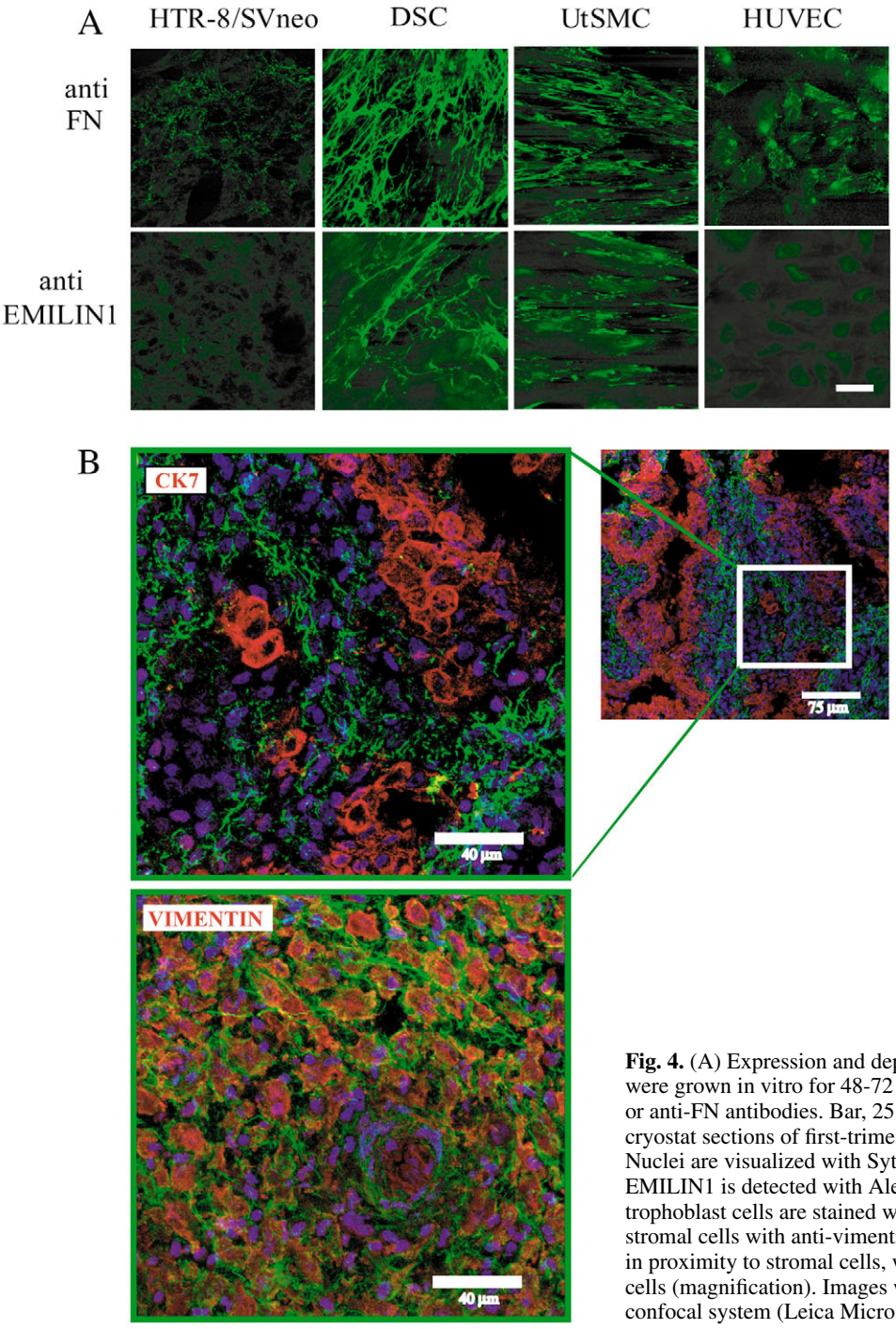

Transmigration of trophoblasts through a stromal cell layer

To support our immunohistochemical and preliminary functional observations, we investigated whether EMILIN1 expressed in vitro by DSC also represented a migratory substrate. For this purpose, stromal cells were plated on the surface of the inserts and grown to confluence for 72 hours. The inserts were then placed in the wells and HTR-

Fig. 4. (A) Expression and deposition of EMILIN1 and FN in vitro. Cells were grown in vitro for 48-72 hours, fixed and stained with anti-EMILIN1 or anti-FN antibodies. Bar, 25 μm. (B). Confocal images obtained from cryostat sections of first-trimester placenta using triple-labeling staining. Nuclei are visualized with Sytox Green and pseudocoloured in blue, EMILIN1 is detected with Alexa Fluor® 633 and pseudocolored in green, trophoblast cells are stained with anti-cytokeratin 7 (red, upper panel), and stromal cells with anti-vimentin (red, lower panel). EMILIN1 is deposited in proximity to stromal cells, whereas it seems absent near to trophoblast cells (magnification). Images were acquired with a Leica TCS SP2 confocal system (Leica Microsystems Heidelberg).

8/SVneo cells were added to the upper chamber and allowed to migrate for 5 hours. DSC did not migrate across the filter pores when either plated alone or when HTR-8/SVneo cells were also added (Fig. 5A). By contrast, HTR-8/SVneo cells displayed a high directional motility when stromal cells were grown on the lower surface of the membranes ($P<0.002$; a representative field of the upper and lower side of the filter is shown in Fig. 5B). The quantitative analysis indicated that nearly 50% of HTR-8/SVneo cells were able to transmigrate under these experimental conditions (Fig. 5B). The presence of specific function-blocking antibodies was able to reduce the migratory process: the inhibition was up to 45% with anti-α4 integrin chain mAb and up to 65% with the anti-β1 integrin chain mAb (Fig. 5C). The use of anti-EMILIN1 mAb 1H2G8 (Spessotto et al., 2003a) produced a reduction of 65% and the simultaneous addition of anti-α4 and anti-EMILIN1 mAbs was responsible for an inhibition as high as 82%. Freshly isolated EVT displayed a similar behaviour: the use of anti-α4 chain and anti-EMILIN1 reduced their migratory ability. Since DSC were shown to produce both FN and EMILIN1 (Fig. 4, supplementary material Fig. S3A), we cannot formally exclude that FN also contributed in part to the haptotactic migration of HTR-8/SVneo cells. Gene silencing was then used to confirm that EMILIN1 was important for trophoblast cell migration. The efficiency of EMILIN1 gene silencing was partial and evident only at 48 hours in our targeted stromal cells (Fig. 5D, upper panel). ECM proteins usually take approximately 48-72 hours to be deposited and adequately organized and we noticed a decrease in migrated cells in areas where EMILIN1 was produced in lower amounts, as shown in the images reported in Fig. 5D (lower panel). Overall, the inhibitory data with the combination of mAbs and the use of siRNA suggested that EMILIN1 plays a crucial role among ECM molecules in directional movement of trophoblast, and indicates that this motility is largely dependent on ligation of deposited EMILIN1 interacting with the α4β1 integrin expressed on trophoblast.

MMP involvement in trophoblast migration

The role of MMPs in trophoblast invasion has been well documented, with the suggestion that they could affect migratory processes of these cells (Nardo et al., 2003). Among the multiple MMPs produced by human placenta, MMP-2 and MMP-9 have been assigned a key role in promoting the invasive capacity of cytotrophoblasts (Campbell et al., 2003). To further elucidate the physiological meaning of our findings we also evaluated a possible function of MMPs in the contest of the haptotactic process involving EMILIN1 and trophoblast cells. Under normal resting culture conditions HTR-8/SVneo cells secreted MMP-9, whereas DSC secreted MMP-2 (supplementary material Fig. S4A, lane1). Both types of cells were able to express MMP-1 (supplementary material Fig. S4A, middle panel, lane 1) and membrane type I (MT1)-MMP (supplementary material Fig. S4A, lower panel, lane 1). The secretion of tissue inhibitor of metalloproteinase-1 (TIMP-1) or TIMP-2 was almost undetectable in both types of cells (data not shown).

Since the cells could modulate the expression of MMPs in the presence of soluble stimulating agents [i.e. 12-O-Tetradecanoylphorbol 13 acetate (TPA) or tumor necrosis factor (TNF)-α] such as MMP-3 and MMP-11 produced by DSC and HTR-8/SVneo cells, respectively (supplementary material Fig. S4A, middle panel, lanes 2 and 3), we asked whether such changes may also be observed in particular culture conditions resembling the in vivo situation. MT1-MMP is the well-known activator of MMP-2 (Seiki, 1999). When HTR-8/SVneo cells were plated on a DSC monolayer, a significant increase ($P=0.002$) in the activity of MT1-MMP in co-cultured cells was found (Fig. 6A, lower panel). Accordingly, the membrane-bound active form of MMP-2 increased, whereas the enzyme in the supernatants decreased (Fig. 6A, upper panel).

To verify whether MMPs played any role in the context of trophoblast migration, first haptotaxis of HTR-8/SVneo cells towards FN or EMILIN1 was performed in the presence of a pan-MMP inhibitor, GM6001. Migration towards FN or gC1q1 was only slightly affected by the presence of GM6001, being more evident at the beginning and less effective during the migratory process towards gC1q1, whereas it was more effective at later times in cells migrating towards FN (supplementary material Fig. S4B). The migration of DiI-labeled HTR-8/SVneo cells towards FN or gC1q1 was then evaluated in the presence of an equal number of DSC (Fig. 6B). As demonstrated for the upregulation of MT1-MMP activity in co-cultured cells (Fig. 6A), the migration of HTR-8/SVneo cells was strongly and significantly reduced ($P<0.01$) by GM6001 only towards gC1q1 but not towards FN. That the presence of DSC is a determining factor was demonstrated by the fact that reducing their number to one-third rendered the GM6001-inhibitory effect less evident (data not shown).

Discussion

An adequate perfusion of the placenta by maternal blood is dependent upon optimal migration and invasion of EVT cells into the decidua, followed by a remodeling of the uteroplacental arteries. The present study used ex vivo EVT and an immortalized human EVT cell line with phenotypic and functional characteristics of EVT to investigate the nature of the receptor-ligand interaction underlying this migratory function of trophoblast cells. To elucidate the role of ECM constituents in the trophoblast-invasion phenomenon, we have: (a) mapped the distribution of ECM constituents in several representative human placenta; (b) examined the ability of these proteins to promote attachment and migration of the HTR-8/SVneo human EVT cell line and of freshly purified EVT cells; (c) used function-perturbing antibodies and siRNA in conjunction with in vitro models of invasion to determine whether EMILIN1 is responsible for mediating migration and invasion. The present study extends a recent finding of a gene-expression study in which the presence of EMILIN1 mRNA was demonstrated in placental tissue (Chen and Aplin, 2003) and demonstrates deposition of EMILIN1 in the decidual stroma. Despite the fact that several substrates were expressed in the stroma, only EMILIN1 displayed gradients with increasing expression towards some unmodified vessels. EMILIN1 strongly promoted cell adhesion and migration of trophoblast cells. Strikingly, directional haptotaxis was much more efficient towards EMILIN1 compared with FN. This finding, along with the observation that DSC produce EMILIN1 in vitro led us to hypothesize that deposited EMILIN1 in the uterine tissue favors the invasion of the uterine wall by trophoblast cells. The important role of DSC inferred by our immunohistochemical data was strongly corroborated

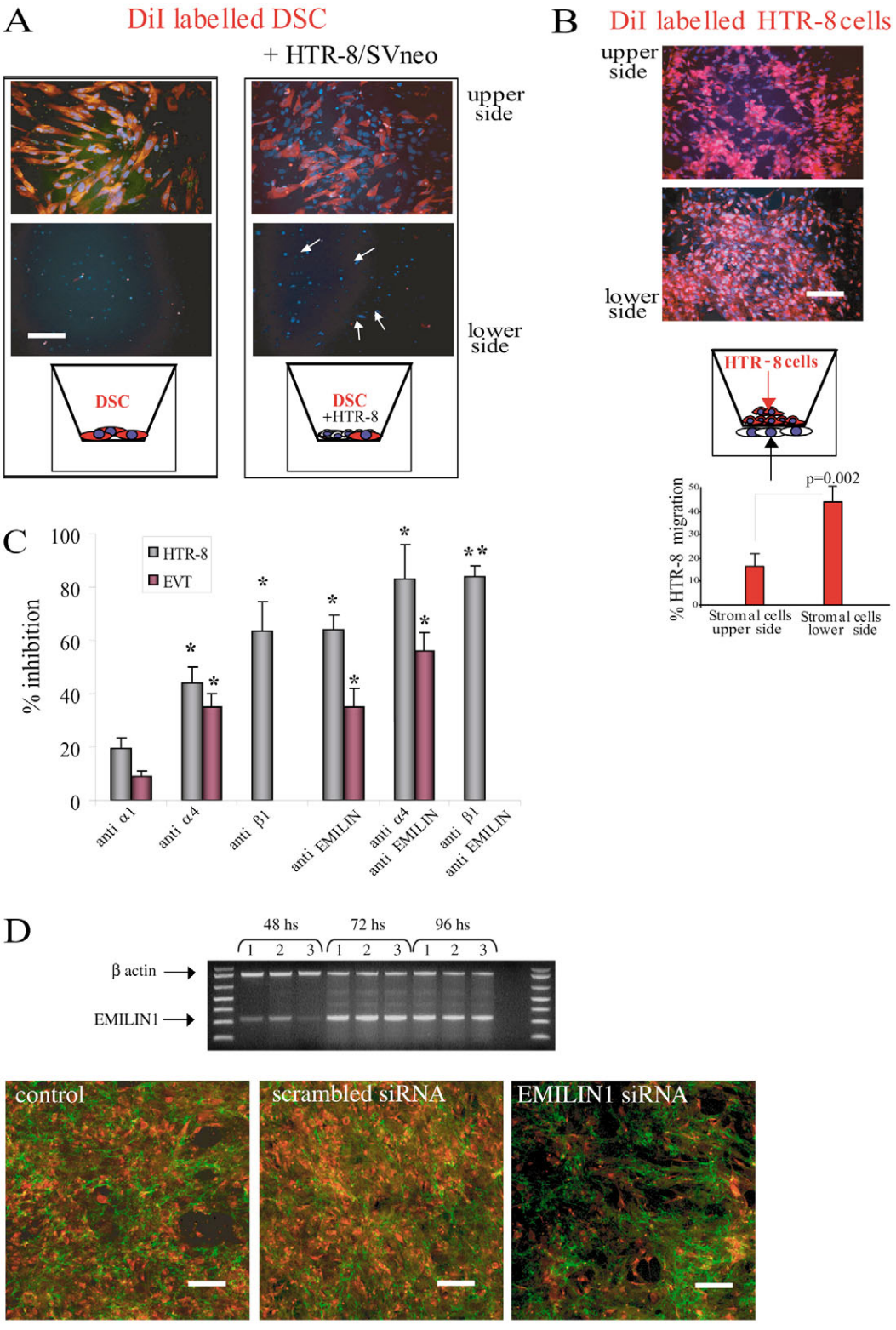

Fig. 5. Transmigration of HTR-8/SVneo through a stromal cell layer. (A) DiI-labeled DSC were plated on the upper side of the filters and allowed to attach. Their spontaneous migration was evaluated before (left side) or after (right side) the addition of unstained HTR-8/SVneo cells. The migration was stopped after 5 hours and the filters were stained with the nuclear dye Hoechst 33342. DSC did not migrate at all (note the absence of red color on the lower part of the filters). The white arrows indicate the nuclei of migrated HTR-8/SVneo cells. Bar, 75 μm. (B) DSC were plated on the lower side of an inverted FluoBlok insert and incubated for 72 hours. The insert was then placed in the chamber and HTR-8/SVneo cells labeled with DiI were added on the upper side. The chambers for migration are schematically represented in the figure. Quantification of HTR-8/SVneo cells migrated through DSC grown on the upper or lower side of the filter is reported in the graph. When DSC were grown on the lower side of the filter, HTR-8/SVneo cell migration was significantly higher than that observed with DSC monolayer in the upper side of the insert. Bar, 75 μm. (C) Inhibition of HTR-8/SVneo and EVT cell transmigration. In some instances, anti-gC1q1 or anti-α4 integrin subunit antibodies were added alone or together to block cell transmigration with DSC monolayer on the lower side of the filter. Anti-α1 integrin subunit antibody was used as negative inhibition control. Data are expressed as mean ± s.d. of four experiments under baseline conditions (mAb anti-α1). Post-hoc comparison of mAb anti-α1 versus specific antibodies after significant ANOVA for repeated-measures main effect, Dunnet's test. *P<0.05, **P<0.01. (D) HTR-8/SVneo cell transmigration under EMILIN1 gene silencing conditions. Upper panel: decidual stromal cell EMILIN1 mRNA levels (30 amplification cycles) at 48, 72 and 96 hours after transfection with the siRNA-specific SMARTpool. Lane 1: control, lipofectamine-treated cells; lane 2: scrambled siRNA; lane 3: EMILIN1 siRNA. RT-PCR analysis reveals that the levels of EMILIN1 mRNA decrease only at 48 hours. Lower panel: evaluation of HTR-8/SVneo cell transmigration after the EMILIN1 gene silencing in decidual stromal cell. The three confocal images, concerning different fields of FluoroBlok inserts, represent the staining of EMILIN1 (in green) produced by decidual stromal cells treated with lipofectamine, transfected with scrambled siRNA or with EMILIN1 siRNA and cultured on the lower side of a FluoBlok filter for 48 hours. Fast DiI-labeled HTR-8/SVneo (in red) were fixed after 7 hours of migration. Bars, 100 μm.

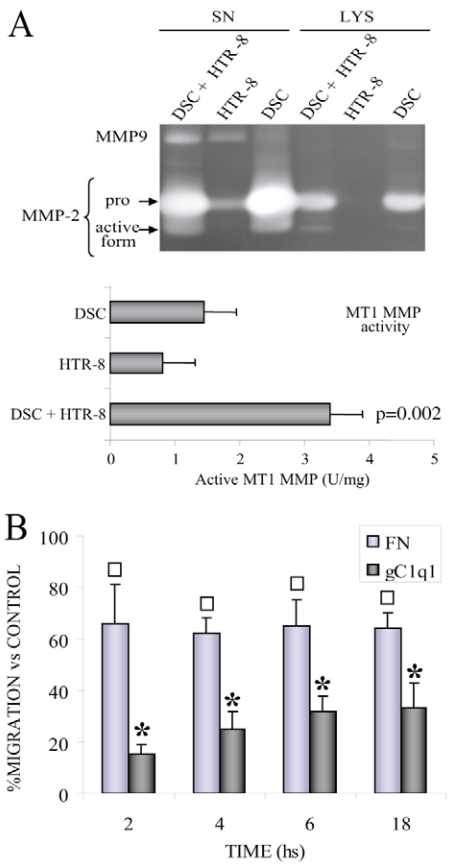

Fig. 6. Production of MMPs in co-cultures. (A) Zymography of conditioned media obtained from co-cultures of DSC and HTR-8/SVneo cells. HTR-8/SVneo cells were added to wells of DSC monolayers. The conditioned media were collected after 24 hours and analysed by zymography. The cells were lysed and loaded for zymography or assayed for MT1-MMP activity. Quantitative determination of total MT1-MMP was performed using the Biotrak MT1-MMP activity assay system (Amersham Biosciences Europe, Orsay, France) according to the manufacturer's instructions. Equal amounts of HTR-8/SVneo and DSC cells were cultivated alone and then processed for zymography and MT1-MMP activity. The increase in MT1-MMP activity in co-cultures was significantly higher (P=0.002) than the summed activity of the enzyme produced by DSC and HTR-8/SVneo cells. (B) Inhibition of haptotaxis. GM6001 (10 μM) was added to block migration of DiI-labeled HTR-8/SVneo cells in the presence of an equal number of DSC. HTS FluoroBlok™ inserts were previously coated underside with gC1q1 or FN. The migratory process was evaluated at different times (2, 4, 6 and 18 hours). P values were determined versus control samples. Open squares, P>0.05; asterisks, P<0.01.

by the quantitative functional data on directional transmigration of HRT-8/SVneo cells in vitro. The strong inhibition of trophoblast cells' movements towards the gradient of EMILIN1 deposited by DSC obtained with the function-blocking anti-EMILIN1 mAb supports the notion that EMILIN1 is largely responsible for the directional motility of trophoblast cells. The formation of a gradient of deposited EMILIN1 by DSC on the inserts is only intuitive since it was not formally demonstrated. However, the nearly threefold higher transmigration of HTR-8/SVneo cells when DSC were grown on the lower surface of the membrane of the inserts compared with the migration obtained when DSC formed a layer on the upper surface is in accord with our hypothesis.

Our data point to a relevant role of the α4β1 integrin receptor in this EMILIN1-dependent trophoblast migration. Since α4β1 exhibits a predominantly leukocyte expression pattern (Rose et al., 2002), the finding that trophoblast cells (HTR-8/SVneo and EVT) could attach to and very efficiently move towards EMILIN1 through α4β1 without any prior artificial cellular activation was unexpected. It has been reported that EVT cells migrating out of chorionic villi selectively express α5β1 integrin and that treatment of EVT cells with an anti-α5β1-integrin-blocking antibody (MacPhee et al., 2001) caused an almost complete inhibition of migration. This finding implied that FN and α5β1 might represent the prevalent ligand-receptor pair involved in the initial anchoring of trophoblast cells in the columns and in the subsequent migration within the uterine wall. α5 and β1 integrins are concentrated at the local outgrowths, as is FN, which is abundant at corresponding sites in vivo (Chen and Aplin, 2003) (present report). Other FN receptors, including those of the αv integrin subfamily and α4β1 were examined, but levels were very low and considered not relevant in the invasion process (Miyamoto et al., 1998). Our results are not in disagreement with the reported migration-stimulating effects of FN. However, EMILIN1, which is not produced by EVT cells, seems to provide a more efficient substrate than FN for EVTs, and it is used by these cells for haptotaxis through the α4β1 integrin receptor.

Cooperation of MMPs with integrins in order to better direct cellular migration could play a contributing role (Deryugina et al., 2001). The ligation of α4β1 integrin upregulated MT1-MMP and conferred a migratory phenotype to mesenchymal cells (Pender et al., 2000). MT1-MMP is a type I membrane-anchored MMP that has been shown to play a crucial role in the pericellular degradation of connective tissue matrix by directly hydrolyzing native collagen (Hotary et al., 2003) and indirectly by initiating a cascade of zymogen activation at the cell surface, which leads to the generation of active MMP-2, MMP-13 and MMP-9 (Strongin et al., 1995; Cowell et al., 1998). A strong upregulation of MT1-MMP was detected only when HTR-8/SVneo cells were co-cultured with DSC. When HTR-8/SVneo cells were present alone in the system we could demonstrate only a partial effect of the general MMP inhibitor GM6001 on cell haptotaxis. Interestingly, this inhibition is more evident for EMILIN1 at one-hour migration, whereas it is stronger when cells move towards FN at 4 hours, suggesting that both ligands might be involved in the invasion process but with a sequential role. However, when labeled HTR-8/SVneo cells migrated in the presence of DSC cells a significant reduction in haptotaxis by GM6001 was detected only towards gC1q1 but not towards FN, linking α4-integrin activation, EMILIN1 ligands as well as MMPs as a part of an interrelated phenomenon that facilitates trophoblast motility.

Our working hypothesis is depicted in Fig. 7: the upregulated and newly released MT1-MMP (60 kDa form) is directed towards MMP-2 produced by DSC in order to activate this enzyme. The active MMP-2 does not cleave EMILIN1 that is processed by other enzymes present in placental tissue, such as plasmin (C.D. et al., unpublished). MMP-2 might instead unmask cryptic sites within the molecule and in this way

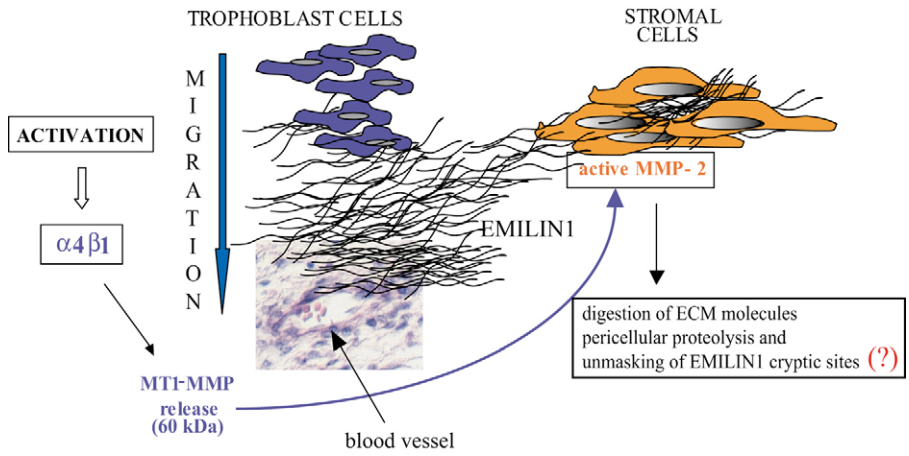

Fig. 7. Schematic representation for the proposed mechanism in the migratory process involving trophoblast cells. The interaction of the gC1q1 domain of EMILIN1, produced by decidual stromal cells, with α4β1 promotes trophoblast migration towards the vessels. The engagement of α4β1 also promotes the release from trophoblast cells of MT1-MMP (60 kDa form) that in turn activates MMP-2 on the membrane of stromal cells. The activated enzyme could digest the ECM component of blood vessels (i.e. laminins), exert an improved efficiency in binding capability or signaling functions of the α4β1 receptor, or unmask EMILIN1 cryptic sites in order to facilitate the migratory phenotype of trophoblast cells. The potential role of FN and other ECM molecules and of integrins other than α4β1 is not represented for clarity.

facilitate the migration process. Alternatively, it might involve cell membrane receptors of the integrin and/or of a different kind in order to create a suitable environment for trophoblast migration. This mechanism has to be validated by further studies to better define the targets of MMP proteolysis and the unique crosstalk with the α4β1 receptor in EMILIN1-mediated migration.

Materials and Methods

Antibodies and other reagents

Function-blocking mAbs to specific integrins were obtained as follows: anti-α1 (clone FB12) and anti-α4 (clone P1H4) from Chemicon International (Temecula, CA), and anti-β1 (clone 4B4) from Coulter/Immunotech (Marseille, France). Anti-paxillin and anti-PECAM-1 (CD31) were purchased from Chemicon; mAb anti-FAK was from Transduction Laboratories (Lexington, KY); rabbit polyclonal antibody against von Willebrand Factor (vWF), mAb anti-cytokeratin 7 (OV-TL12/30) and mAb anti-vimentin (clone V9) were from DAKOCytomation (Milan, Italy). mAb anti-HLA class I (W6/32) were provided by Sigma Aldrich (Milan, Italy). Rabbit polyclonal anti-FN was produced by immunization of rabbits with plasma human FN; rabbit polyclonal anti-EMILIN1 (As556) and mouse monoclonal anti-gC1q1 (1H2G8) were obtained as described (Spessotto et al., 2003a). Rabbit polyclonal anti-MT1-MMP and mouse monoclonal anti-MMP-11 antibodies were provided by Chemicon, whereas mouse monoclonal anti-MMP-1 and anti-MMP-3 antibodies were obtained from Oncogene Research Products (Boston, MA).

FN was purchased from Calbiochem-Novabiochem (La Jolla, CA). VN was purified from human plasma. Human skin Col III, placental Col IV, placental Col V, human plasma fibrinogen and high M_r HA were obtained from Sigma; rat tail Col I and matrigel were purchased from BD Biosciences (Bedford, MA). Native LN-1-nidogen complex from Engelbreth-Holm-Swarm (EHS) mouse tumor was obtained as previously described (Engvall et al., 1983). Chick Col VI tetramers were purified as previously described (Mazzucato et al., 1999). Tenascin and human perlecan were kindly provided by Luciano Zardi and Anders Malmström, respectively.

For the production of EMILIN1 293 cells, constitutively expressing EBNA-1 protein (293-EBNA) and secreting EMILIN1 were used. Briefly, polypeptides secreted in the cell supernatant were purified by ion-exchange chromatography on a DEAE-cellulose column (Amersham Pharmacia Biotech) and size-exclusion chromatography using Sepharose CL-4B (1.0×90.0 cm column, Amersham Pharmacia Biotech) as described (Mongiat et al., 2000). The preparation was checked for the presence of LN and FN by immunoblotting with specific antibodies and proved to be nearly devoid of these contaminants. The C-terminal 6His-tagged recombinant fragment of EMILIN1 (gC1q1) was purified by affinity chromatography on Ni-NTA resin (Qiagen GmbH) under native conditions as described (Spessotto et al., 2003a).

The MMP inhibitor GM6001 (Ilomastat) was obtained from Chemicon; TPA and TNF-α from Sigma.

EVT cell line, HTR-8/SVneo

HTR-8/SVneo cell line was provided by Peeyush K. Lala (Dept. of Anatomy and Cell Biology, University of Western Ontario, Canada). The cell line was produced by immortalization of HTR-8 cells, an EVT cell line from primary cultures of cytotrophoblast cells, with SV40 virus (Graham et al., 1993). It expresses the trophoblast-specific cytokeratin 7 (Maldonado-Estrada et al., 2004), as well as cytokeratin 8 and cytokeratin 18; placental-type alkaline phosphatase; high-affinity urokinase-type plasminogen activator receptor; HLA framework antigen W6/32, IGF-II messenger RNA and protein; and a selective repertoire of integrins α1, α3, α5, αv, β1, and VN receptor αvβ3/β5 (Irving and Lala, 1995; Irving et al., 1995). In the present study, cells between 70–90 passages were used and grown in RPMI 1640 supplemented with 10% fetal bovine serum (FBS).

Isolation of fresh EVT and decidual stromal cells

Placenta and decidual specimens were obtained from women undergoing elective termination of pregnancy at 8-12 weeks of gestation. The study was approved by the institutional review board of The Maternal-Children Hospital (IRCCS 'Burlo Garofolo', Trieste, Italy) and informed consent was obtained from all women providing the tissue specimens. In this study we have investigated seven placentas. Fragments of decidual tissue of approximately 1 cm^3 containing some floating and anchoring villi were used for the study of the implantation side. EVTs were purified from placental tissue incubated with Hanks balanced salt solution (HBSS; Invitrogen) containing 0.25% trypsin and 0.2 mg/ml Dnase type I (Roche, Mannheim, Germany) for 20 minutes at 37°C, following a previously published procedure (Tedesco et al., 1993; Bulla et al., 1999). After Percoll gradient fractionation, the contaminating leukocytes were removed by immunomagnetic beads coated with mAb to CD45 (Dynabeads M-450, Dynal, Oxoid, Milan, Italy).

DSCs were isolated from decidual specimens. Briefly, finely minced decidual tissue was digested with collagenase type I (1 mg/ml) (Worthington Biochemical Corporation, DBA, Milan, Italy) for 2 hours at 37°C, filtered through a 100 μm pore filter (BD Biosciences) and further digested with 0.1% trypsin (Sigma) and 0.05% Dnase type I (Roche) for 7 minutes. The cells were grown in RPMI with 10% fetal calf serum (FCS). HUVEC were isolated from three to five normal umbilical cord veins by collagenase digestion as previously reported (Tedesco et al., 1997; Lorenzon et al., 1998). UtSMC were provided with their respective culture media and additives by Cambrex Bio Science (Rockland, ME).

Immunohistochemistry and immunofluorescence staining

First-trimester healthy human placenta tissues were obtained from patients undergoing elective termination of pregnancy at 10-12 weeks of gestation. Fragments of placental tissue of approximately 1 cm^3 were embedded in OCT (Miles Laboratory, Milan, Italy), snap-frozen in liquid nitrogen and kept at –80°C until use. Cryostat sections of approximately 6 μm were air dried, fixed in acetone for 10 minutes at room temperature and either used immediately or kept at –80°C wrapped in aluminum foil. Immunoperoxidase staining was performed on placental sections incubated with the primary antibodies followed by peroxidase-labeled secondary antibodies (EnVision^{TM+} kit, DakoCytomation). Double labeling was performed using Dako EnVision Doublestain System (DakoCytomation). The

enzymatic reactions were developed with diaminobenzidine (DAB) for immunoperoxidase and Fast Red for alkaline phosphatase (ALP). The reaction product of ALP cromogen produce a brilliant red fluorescence that is visible by fluorescence microscopy using a fluorescein filter (Murdoch et al., 1990). Triple labeling was performed adding fluorescein isothiocyanate (FITC)-labeled mAb anti-cytokeratin 7 on the same sections. In some cryostat sections nuclei were visualized with Sytox Green and other structures were detected with Alexa Fluor® 546- and Alexa Fluor® 633-labeled secondary antibodies (Molecular Probes, Eugene, OR) to obtain multiple staining. Images were acquired with a Leica TCS SP2 confocal system (Leica Microsystems Heidelberg, Mannheim, Germany), using the Leica Confocal Software (LCS) and a 40× fluorescence objective on a Leica DM IRE2 microscope.

In vitro immunofluorescence analysis

Multiwell plates or acid-washed coverslips were coated with FN (10 μg/ml), EMILIN1 (10 μg/ml), gC1q1 (20 μg/m1) and VN (10 μg/ml) for 16 hours at 4°C and non-specific binding was blocked with 1% RIA-grade bovine serum albumin (BSA) (Sigma). Cells were then plated onto the various substrates for 30 to 40 minutes as indicated, fixed with 4% (w/v) formaldehyde for 10 minutes, and permeabilized in PBS containing 0.1% Triton X-100 for 2 minutes. The cells were then incubated for 1 hour with primary antibodies in PBS, washed, and further incubated with the appropriate FITC-conjugated secondary antibodies (Amersham Pharmacia Biotech). After extensive washes, coverslips were mounted in Mowiol 4-88 (Calbiochem-Novabiochem) containing 2.5% (w/v) 1,4-diazabicyclo[2,2,2]-octane (DABCO) (Sigma). Images were acquired with a Leica TCS SP2 confocal system, using the LCS and a 63× fluorescence objective on a Leica DM IRE2 microscope.

EMILIN1 gene silencing

For the EMILIN1 expression knockdown the Dharmacon siRNA-specific SMARTpool (Dharmacon, Chicago, IL) was used. The transfection of decidual stromal cells was performed according to the manufacturer's instructions. Steady-state RNA expression levels were analyzed at different cell culture times by semi-quantitative RT/PCR using the SV RNA purification kit (Promega Italia) to isolate total RNA and the access kit (Promega) for RNA retrotranscription and cDNA amplification. To perform PCR, primers designed on distinct exons to distinguish for possible DNA-derived amplification products were used, and gel analysis was done after 25, 30 and 40 amplification cycles to select a cycle number in which the amplification process was linear. β-actin was co-amplified for normalization. Negative controls included scrambled RNA oligos (Dharmacon).

Cell adhesion assay

The quantitative cell adhesion assay used in this study is based on centrifugation and has previously been described (Giacomello et al., 1999; Spessotto et al., 2000). Briefly, six-well strips of flexible polyvinyl chloride-denoted centrifugal assay for fluorescence-based cell adhesion (CAFCA) miniplates, covered with double-sided tape (bottom units), were coated with the different substrates. Cells were labeled with the vital fluorochrome calcein AM (Molecular Probes) for 15 minutes at 37°C and then aliquoted into the bottom CAFCA miniplates, which were centrifuged to synchronize the contact of the cells with the substrate. The miniplates were then incubated for 20 minutes at 37°C and subsequently mounted together with a similar CAFCA miniplate to create communicating chambers for subsequent reverse centrifugation. The relative number of cells bound to the substrate (i.e. remaining in the wells of the bottom miniplates) and cells that fail to bind to the substrate (i.e. remaining in the wells of the top miniplates) was estimated by top/bottom fluorescence detection in a computer-interfaced *SPECTRAFluor* Plus microplate fluorometer (Tecan, Rapperswit, Switzerland). In experiments aimed at examining the effects of blocking antibodies, the various antibodies were added directly to the wells, just before plating the cells.

Cell motility assay

Haptotactic-like migration of HTR-8/SVneo or ETV cells in response to ECM substrates was assessed by fluorescence-assisted transmigration invasion and motility assay (FATIMA) (Spessotto et al., 2000, Spessotto et al., 2003b). The procedure is based on the use of Transwell-like inserts carrying fluorescence-shielding porous polyethylene terephthalate (PET) membranes (polycarbonate-like material with 8 μm pores), HTS FluoroBlok™ inserts (Becton-Dickinson, Falcon, Milan, Italy). Membranes were coated (20-50 μg/ml in 50 μl) on either the upper- or underside with the various ECM molecules in bicarbonate buffer at 4°C overnight and blocked with 1% BSA for 1 hour at room temperature. Cells were fluorescently tagged with the lipophilic dye DiI (Molecular Probes) used at a final concentration of 5 μg/ml for 10-15 minutes at 37°C. The cells were washed, resuspended in RPMI with 0.1% BSA and then added to the upperside of the inserts (2×10^5 cells/insert). In some instances, cells were pre-incubated with blocking antibodies or non-blocking control antibodies and added to the upperside of the FluoroBlok inserts. Migratory behavior of the cells was then monitored at different time-intervals by independent fluorescence detection from the top (corresponding to non-transmigrated cells) and bottom (corresponding to transmigrated cells) side of the membrane using the computer-interfaced *SPECTRAFluor Plus* instrument (Tecan).

Western blotting

For MT1-MMP, MMP-1, MMP-3, and MMP-11, detection-standardized supernatants and/or cell lysates were loaded onto a sodium dodecyl sulfate (SDS)-acrylamide gel (4-15% polyacrylamide), subjected to electrophoresis under reducing conditions and transferred to a nitrocellulose membrane. For ECM production, different adherent cell-types at confluence were treated with 0.1 M NH_4OH for 5 minutes, then extensively washed and the ECM molecules eventually deposited were extracted with SDS sample buffer. These extracts were loaded onto SDS-acrylamide-gels (8% polyacrylamide) under reducing conditions and blotted onto nitrocellulose filters. The membranes were saturated with Tris-buffered saline (TBS) buffer (containing 20 mM TRIS and 0.15 M NaCl) containing 0.1% Tween 20 (TBST) and 5% non-fat dry milk for 2 hours at room temperature and then incubated with primary antibodies at 4°C overnight. After extensive washing in TBST, the membranes were incubated with horseradish peroxidase (HRP)-conjugated appropriate secondary antibodies (Amersham) and then revealed with the ECL Plus chemiluminescence kit (Amersham).

Gelatin zymography

The presence of MMP-2 and MMP-9 in the media was demonstrated by gelatin zymography. The culture media were standardized according to the protein content of cell lysates and were loaded onto SDS-acrylamide-gelatin gels (8% polyacrylamide, 0.1% gelatin). The gels were then washed twice for 30 minutes with 50 mM Tris-HCl (pH 7.4) containing 2.5% Triton X-100, incubated overnight at 37°C in 50 mM Tris-HCl (pH 7.4), containing 150 mM NaCl and 10 mM $CaCl_2$, stained for 30 minutes with 30% methanol/10% acetic acid containing 0.5% Coomassie Brilliant Blue R-250, destained, and finally photographed.

Statistical evaluation

Statistical significance of the results was determined by using the Student's *t*-test. A value of $P<0.05$ was considered to be significant. Mean ± s.d. values of three to five experiments are presented. For some experiments, data were subjected to repeated-measures analysis of variance (ANOVA), followed when appropriate by a post-hoc Dunnet's test.

We thank F. De Seta, E. Bianchini and A. Candiotto of the Department of Reproductive and Developmental Sciences for providing the placenta samples and E. Bidoli for helping in statistical analyses. Financial support was provided by AIRC (A.C. and F.T.), FSN (A.C.), the European NoE 'EMBIC' within FP6 (contract number LSHN-CT-2004-512040), Fondo Italiano per la Ricerca di Base (FIRB, A.C. and F.T.) and COFIN 2003 provided by Ministero dell'Istruzione, Università e Ricerca (MIUR) to F.T.

References

Aplin, J. D. (1993). Expression of integrin α6β4 in human trophoblast and its loss from extravillous cells. *Placenta* **14**, 203-215.

Aplin, J. D., Haigh, T., Lacey, H., Chen, C. P. and Jones, C. J. (2000). Tissue interactions in the control of trophoblast invasion. *J. Reprod. Fertil. Suppl.* **55**, 57-64.

Braghetta, P., Ferrari, A., de Gemmis, P., Zanetti, M., Volpin, D., Bonaldo, P. and Bressan, G. M. (2002). Expression of the EMILIN-1 gene during mouse development. *Matrix Biol*. **21**, 603-609.

Bulla, R., de Guarrini, F., Pausa, M., Fischetti, F., Meroni, P. L., De Seta, F., Guaschino, S. and Tedesco, F. (1999). Inhibition of trophoblast adhesion to endothelial cells by sera of women with recurrent spontaneous abortions. *Am. J. Reprod. Immunol*. **42**, 116-123.

Bulla, R., Villa, A., Bossi, F., Cassetti, A., Radillo, O., Spessotto, P., De Seta, F., Guaschino, S. and Tedesco, F. (2005). VE-cadherin is a critical molecule for trophoblast-endothelial cell interaction in decisula spiral arteries. *Exp. Cell Res.* **303**, 101-113.

Campbell, S., Rowe, J., Jackson, C. J. and Gallery, E. D. (2003). In vitro migration of cytotrophoblasts through a decidual endothelial cell monolayer: the role of matrix metalloproteinases. *Placenta* **24**, 306-315.

Chen, C. P. and Aplin, J. D. (2003). Placental extracellular matrix: gene expression, deposition by placental fibroblasts and the effect of oxygen. *Placenta* **24**, 316-325.

Colombatti, A., Doliana, R., Bot, S., Canton, A., Mongiat, M., Mungiguerra, G., Paron-Cilli, S. and Spessotto, P. (2000). The EMILIN protein family. *Matrix Biol*. **19**, 289-301.

Cowell, S., Knauper, V., Stewart, M. L., D'Ortho, M. P., Stanton, H., Hembry, R. M., Lopez-Otin, C., Reynolds, J. J. and Murphy, G. (1998). Induction of matrix metalloproteinase activation cascades based on membrane-type 1 matrix metalloproteinase: associated activation of gelatinase A, gelatinase B and collagenase 3. *Biochem. J.* **331**, 453-458.

Damsky, C. H., Fitzgerald, M. L. and Fisher, S. J. (1992). Distribution patterns of extracellular matrix components and adhesion receptors are intricately modulated

during the first trimester cytotrophoblast differentiation along the invasive pathway, in vivo. *J. Clin. Invest.* **89**, 210-222.

Deryugina, E. I., Ratnikov, B., Monosov, E., Postnova, T. I., DiScipio, R., Smith, J. W. and Strongin, A. Y. (2001). MT1-MMP initiates activation of pro-MMP-2 and integrin alphavbeta3 promotes maturation of MMP-2 in breast carcinoma cells. *Exp. Cell Res.* **263**, 209-223.

Doliana, R., Mongiat, M., Bucciotti, F., Giacomello, E., Deutzmann, R., Volpin, D., Bressan, G. M. and Colombatti, A. (1999). EMILIN, a component of the elastic fiber and a new member of the C1q/tumor necrosis factor superfamily of proteins. *J. Biol. Chem.* **274**, 16773-16781.

Engvall, E., Krusius, T., Wewer, U. and Ruoslahti, E. (1983). Laminin from rat yolk sac tumor: isolation, partial characterization, and comparison with mouse laminin. *Arch. Biochem. Biophys.* **222**, 649-656.

Even-Ram, S., Uziely, B., Cohen, P., Grisaru-Granovsky, S., Maoz, M., Ginzburg, Y., Reich, R., Vlodavsky, I. and Bar-Shavit, R. (1998). Thrombin receptor overexpression in malignant and physiological invasion processes. *Nat. Med.* **4**, 909-914.

Giacomello, E., Neumayer, J., Colombatti, A. and Perris, R. (1999). Centrifugal assay for fluorescence-based cell adhesion adapted to the analysis of ex vivo cells and capable of determining relative binding strengths. *Biotechniques* **26**, 758-762, 764-766.

Graham, C. H. and Lala, P. K. (1992). Mechanisms of placental invasion of the uterus and their control. *Biochem. Cell Biol.* **70**, 867-870.

Graham, C. H., Hawley, T. S., Hawley, R. G., MacDougall, J. R., Kerbel, R. S., Khoo, N. and Lala, P. K. (1993). Establishment and characterization of first trimester human trophoblast cells with extended life span. *Exp. Cell Res.* **206**, 204-211.

Hamilton, G. S., Lysiak, J. J., Han, V. K. M. and Lala, P. K. (1998). Autocrine-paracrine regulation of human trophoblast invasiveness by insulin-like growth factor (IGF)-II and IGF-binding protein (IGFBP)-1. *Exp. Cell Res.* **244**, 147-156.

Hotary, K. B., Allen, E. D., Brooks, P. C., Datta, N. S., Long, M. W. and Weiss, S. J. (2003). Membrane type I matrix metalloproteinase usurps tumor growth control imposed by the three-dimensional extracellular matrix. *Cell* **114**, 33-45.

Ilic, D., Genbacev, O., Jin, F., Caceres, E., Almeida, E. A., Bellingard-Dubouchaud, V., Schaefer, E. M., Damsky, C. H. and Fisher, S. J. (2001). Plasma membrane-associated pY397FAK is a marker of cytotrophoblast invasion in vivo and in vitro. *Am. J. Pathol.* **159**, 93-108.

Irving, J. A. and Lala, P. K. (1995). Functional role of cell surface integrins on human trophoblast cell migration: regulation by TGF-ß, IGF-II, and IGFBP-1. *Exp. Cell Res.* **217**, 419-427.

Irving, J. A., Lysiak, J. J., Graham, C. H., Hearn, S., Han, V. K. and Lala, P. K. (1995). Characteristics of trophoblast cells migrating from first trimester chorionic villus explants and propagated in culture. *Placenta* **16**, 413-433.

Kaufmann, P. and Castellucci, M. (1997). Extravillous trophoblast in the human placenta. *Trophoblast Res.* **10**, 21-65.

Kilburn, B. A., Wang, J., Duniec-Dmuchkowski, Z. M., Leach, R. E., Romero, R. and Armant, D. R. (2000). Extracellular matrix composition and hypoxia regulate the expression of HLA-G and integrins in trophoblast cell line. *Biol. Reprod.* **62**, 739-747.

Korhonen, M., Ylanne, J., Laitinen, L., Cooper, H. M., Quaranta, V. and Virtanen, I. (1991). Distribution of the α1-6 integrin subunits in human developing and term placenta. *Lab. Invest.* **65**, 347-356.

Lorenzon, P., Vecile, E., Nardon, E., Ferrero, E., Harlan, J. M., Tedesco, F. and Dobrina, A. (1998). Endothelial cell E- and P-selectin and vascular cell adhesion molecule- 1 function as signaling receptors. *J. Cell Biol.* **142**, 1381-1391.

MacPhee, D. J., Mostachfi, H., Han, R., Lye, S. J., Post, M. and Caniggia, I. (2001). Focal adhesion kinase is a key mediator of human trophoblast development. *Lab. Invest.* **81**, 1469-1483.

Maldonado-Estrada, J., Menu, E., Roques, P., Barré-Sinoussi, F. and Chaouat, G. (2004). Evaluation of Cytokeratin 7 as an accurate intracellular marker with which to assess the purify of human placental villous trophoblast cells by flow cytometry. *J. Immunol. Methods* **286**, 21-34.

Mazzucato, M., Spessotto, P., Masotti, A., De Appollonia, L., Cozzi, M. R., Yoshioka, A., Perris, R., Colombatti, A. and De Marco, L. (1999). Identification of domains responsible for von Willebrand factor type VI collagen interaction mediating platelet adhesion under high flow. *J. Biol. Chem.* **274**, 3033-3041.

McCarthy, J. B. and Furcht, L. T. (1984). Laminin and fibronectin promote the haptotactic migration of B16 mouse melanoma cells in vitro. *J. Cell Biol.* **98**, 1474-1486.

Miyamoto, S., Katz, B. Z., Lafrenie, R. M. and Yamada, K. M. (1998). Fibronectin and integrins in cell adhesion, signaling, and morphogenesis. *Ann. N. Y. Acad. Sci.* **857**, 119-129.

Mongiat, M., Mungiguerra, G., Bot, S., Mucignat, M. T., Giacomello, E., Doliana, R. and Colombatti, A. (2000). Self-assembly and supramolecular organization of EMILIN. *J. Biol. Chem.* **275**, 25471-25480.

Murdoch, A., Jenkinson, E. J., Johnson, G. D. and Owen, J. J. T. (1990). Alkaline phosphatase-fast red, a new fluorescent label: Application in double labelling for cell surface antigen and cell cycle analysis. *J. Immunol. Methods* **132**, 45-49.

Nardo, L. G., Nikas, G. and Makrigiannakis, A. (2003). Molecules in blastocyst implantation. Role of matrix metalloproteinases, cytokines and growth factors. *J. Reprod. Med.* **48**, 137-147.

Norwitz, E. R., Schust, D. J. and Fisher, S. J. (2001). Implantation and the survival of early pregnancy. *N. Engl. J. Med.* **345**, 1400-1408.

Pender, S. L., Salmela, M. T., Monteleone, G., Schnapp, D., McKenzie, C., Spencer, J., Fong, S., Saarialho-Kere, U. and MacDonald, T. T. (2000). Ligation of alpha4ss1 integrin on human intestinal mucosal mesenchymal cells selectively up-regulates membrane type-1 matrix metalloproteinase and confers a migratory phenotype. *Am. J. Pathol.* **157**, 1955-1962.

Queenan, J. T., Jr, Kao, L. C., Arboleda, C. E., Ulloa-Aguirre, A., Golos, T. G., Cines, D. B. and Strauss, J. F. D. (1987). Regulation of urokinase-type plasminogen activator production by cultured human cytotrophoblasts. *J. Biol. Chem.* **262**, 10903-10906.

Rose, D. M., Han, J. and Ginsberg, M. H. (2002). Alpha 4 integrins and the immune response. *Immunol. Rev.* **186**, 118-124.

Seiki, M. (1999). Membrane-type matrix metalloproteinases. *Acta Pathol. Microbiol. Immunol. Scand.* **107**, 137-143.

Spessotto, P., Giacomello, E. and Perris, R. (2000). Fluorescence assays to study cell adhesion and migration in vitro. *Methods Mol. Biol.* **139**, 321-343.

Spessotto, P., Cervi, M., Mucignat, M. T., Mungiguerra, G., Sartoretto, I., Doliana, R. and Colombatti, A. (2003a). beta 1 integrin-dependent cell adhesion to EMILIN-1 is mediated by the gC1q domain. *J. Biol. Chem.* **278**, 6160-6167.

Spessotto, P., Gronkowska, A., Deutzmann, R., Perris, R. and Colombatti, A. (2003b). Preferential locomotion of leukemic cells towards laminin isoforms 8 and 10. *Matrix Biol.* **22**, 351-361.

Strongin, A. Y., Collier, I., Bannikov, G., Marmer, B. L., Grant, G. A. and Goldberg, G. I. (1995). Mechanism of cell surface activation of 72-kDa type IV collagenase. Isolation of the activated form of the membrane metalloprotease. *J. Biol. Chem.* **270**, 5331-5338.

Tedesco, F., Narchi, G., Radillo, O., Meri, S., Ferrone, S. and Betterle, C. (1993). Susceptibility of human trophoblast to killing by human complement and the role of the complement regulatory proteins. *J. Immunol.* **151**, 1562-1570.

Tedesco, F., Pausa, M., Nardon, E., Introna, M., Mantovani, A. and Dobrina, A. (1997). The cytolytically inactive terminal complement complex activates endothelial cells to express adhesion molecules and tissue factor procoagulant activity. *J. Exp. Med.* **185**, 1619-1627.

Zhou, Y., Fisher, S., Janatpour, M., Genbacev, O., Dejana, E., Wheelock, M. and Damsky, C. (1997). Human cytotrophoblasts adopt a vascular phenotype as they differentiate. A strategy for successful endovascular invasion? *J. Clin. Invest.* **99**, 2139-2151.